Development Administration and by the National Science Foundation.

[a]Present address: Physics Department, Columbia University, New York, N. Y. 10027.

[1]H. Cheng and T. T. Wu, Phys. Rev. 183, 1324 (1969).
[2]J. D. Bjorken *et al.*, Phys. Rev. D 1, 1382 (1971).
[3]H. T. Nieh, Phys. Lett. 38B, 100 (1972).
[4]L. Ahrens *et al.*, Phys. Rev. Lett. 31, 131 (1973), and Phys. Rev. D 9, 1894 (1974).
[5]For a summary, see G. Wolf, in *Proceedings of the International Symposium on Lepton and Photon Interactions at High Energies, Stanford, California, 1975*, edited by W. T. Kirk (Stanford Linear Accelerator Center, Stanford, California, 1975), p. 795.
[6]P. G. Freund, Nuovo Cimento 48A, 541 (1967).
[7]K. Moffeit, in *Proceedings of the Sixth International Symposium on Electron and Photon Interactions at High Energies*, edited by H. Rollnik and W. Pfeil (North-Holland, Amsterdam, 1974), p. 313.
[8]A. Browman *et al.*, Phys. Rev. Lett. 20, 1313 (1975).
[9]K. Schilling and G. Wolf, Nucl. Phys. B61, 381 (1973).
[10]J. Ballam *et al.*, Phys. Rev. D 7, 3150 (1973).
[11]R. Erbe *et al.*, Phys. Rev. 175, 1669 (1968), and 188, 2060 (1969).
[12]R. L. Anderson *et al.*, Phys. Rev. D 1, 27 (1970).
[13]H. Alvensleben *et al.*, Phys. Rev. Lett. 28, 66 (1972).
[14]C. Berger *et al.*, Phys. Lett. 39B, 659 (1972).
[15]R. L. Anderson *et al.*, Phys. Rev. Lett. 30, 149 (1973).
[16]H. J. Besch *et al.*, Nucl. Phys. B70, 257 (1974).
[17]H. J. Behrend *et al.*, Phys. Lett. 56B, 408 (1975).

Dimuon and Trimuon Final States in Deep Inelastic Muon Scattering

C. Chang and K. Wendell Chen
Michigan State University, East Lansing, Michigan 48824

and

A. Van Ginneken
Fermi National Accelerator Laboratory, Batavia, Illinois 60510

(Received 4 April 1977)

32 dimuon and 11 trimuon events are observed in deep inelastic muon interactions at 150 GeV. The rate of diumuon production is greater than 5×10^{-4} that of inclusive muon scattering. High-inelasticity trimuons occur at a rate one order of magnitude lower. These events are more numerous and the extra muons have qualitatively different production characteristics than muons expected from conventional sources.

Multimuon events are observed[1] in a data sample of an experiment on deep inelastic muon-nucleon interactions at 150 GeV.[2,3] Production rates and characteristics are inconsistent with either π and K decays or quantum electrodynamical (QED) tridents being the source of these muons. The assumption that production of "direct" muons by virtual photons is similar to that observed in hadron-hadron interactions leads to prediction too low by two orders of magnitude.

Processes yielding one extra muon (2μ) in the final state ($\mu N \to \mu\mu X$) are observed at a rate slightly larger than 5×10^{-4} per deep inelastic muon-scattering event. The acceptance of the apparatus is approximately such that the muons must have an energy larger than 17 GeV and an angle larger than 13 mrad. In addition, the events should not be accompanied by a penetrating charged particle at an angle less than 13 mrad. Events with three muons (3μ) in the final state ($\mu N \to \mu\mu\mu X$) are found to occur at a rate roughly about 10^{-4} per deep inelastic muon-scattering event. This Letter deals mostly with 2μ events.

The apparatus (Fig. 1) consists of a 194-cm-long (1.57×10^{3} g/cm^2) iron-and-scintillator target followed by three (79 cm long, 173 cm diameter) toroidal iron magnets, interspersed by an array of wire spark chambers. In the central core of the magnets (at radii less than 15.2 cm), the iron is replaced by lead-loaded concrete and the magnetic field effectively vanishes in this region. Likewise at radii below 15.2 cm, there is an inactive region in the spark chambers. Two beam veto counters (30.5 cm in diameter) placed before and after the last magnet reject those events with a penetrating charged particle at a small angle.[1,3]

The present data sample derives from a total of 6.1×10^{9} incident muons (50.9% μ^+, 49.1% μ^-) of 150 GeV. The trigger requirement is for a muon to penetrate all three toroidal magnets and

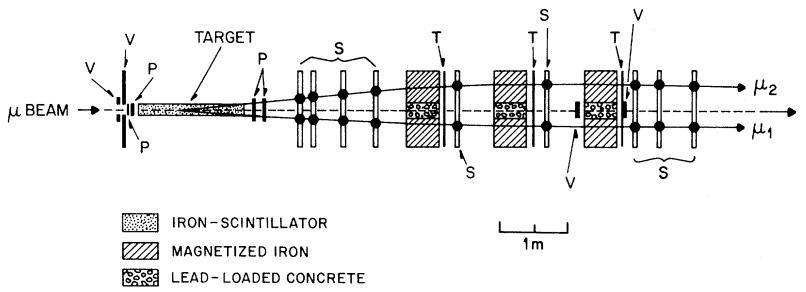

FIG. 1. Layout of apparatus. P denotes proportional chambers, S spark chambers, T trigger counters, and V veto counters.

register in each spark chamber. This corresponds roughly to the energy and angle cuts mentioned above. In the exposure, 25 550 single-μ events are thus registered. The scanning criteria for multimuon events are the following: (1) The muon trajectories (both scattered and produced μ's) extrapolate to the beam track to within 2 cm; (2) muons penetrate the entire target-detector array [this condition is relaxed for trimuon members ($E_{\mu_3} \gtrsim 6$ GeV)]; (3) μ's can be momentum analyzed by at least one magnet; (4) correct timing and hodoscope information for all final-state muons; and (5) the origin of the events must lie within the target. A total of 32 2μ's and 11 3μ's were observed in this manner. In excess of 80% of 2μ events were accompanied by a shower which extends at least through 20 cm of iron as seen by the iron-scintillator target array.

The origin of the multimuons (both as calculated by extrapolating the muon trajectories and as observed in the iron-scintillator target array) is uniform along the beam direction in the target. This discriminates against the possibility that these events are due to the small pion contamination of the muon beam (about 10^{-5} π per μ). Independently of the argument, a calculation based on 150-GeV-pion–induced dimuon data[4] shows this component to be less than 1% of the observed 2μ-event rate. Likewise the charge structure (see below) is inconsistent with a large fraction of the 2μ events being of hadronic origin.

The 43 multimuon events are divided according to charge distribution as follows: (1) for incident μ^+, 10 $\mu^+\mu^-$, 10 $\mu^+\mu^+\mu$, and 4 $\mu^+\mu^+\mu^-$; (2) for incident μ^-, 5 $\mu^-\mu^+$, 7 $\mu^-\mu^-$, and 7 $\mu^-\mu^-\mu^+$. In 2μ events of opposite charge the energy of the scattered muon, E_{μ_1}, is unambiguously determined and always exceeds the energy of the produced muon, E_{μ_2}. This feature is used to identify the scattered and produced muon in pairs of the same charge. The results are shown in Fig. 2. For all 2μ events, $\langle E_{\mu_1}\rangle/\langle E_{\mu_2}\rangle = 2.8$ When the incident-μ^+ and -μ^- events are combined, the produced μ in 2μ events appears equally likely to be of either charge. The charge structure of 3μ events is consistent with produced muons being always of opposite charge.

The assumption which identifies the leading muon as the scattered muon defines the kinematics of the virtual photon. In contrast with neutrino scattering experiments the standard variables associated with the muon-scattering vertex are here readily obtained: $y = \nu/E_\mu$, $q^2 = 4E_\mu E_{\mu_1} \times \sin^2(\theta/2)$, $x = q^2/2M\nu$, and $W^2 = M^2 + 2M\nu - q^2$, where E_μ is the incident muon energy, $\nu = E_\mu - E_{\mu_1}$, M is the nucleon mass, and θ is the scattering angle. Figures 3(a)–(d) show the distribution of the 2μ events for each of the variables defined above. Three 2μ events are not shown in

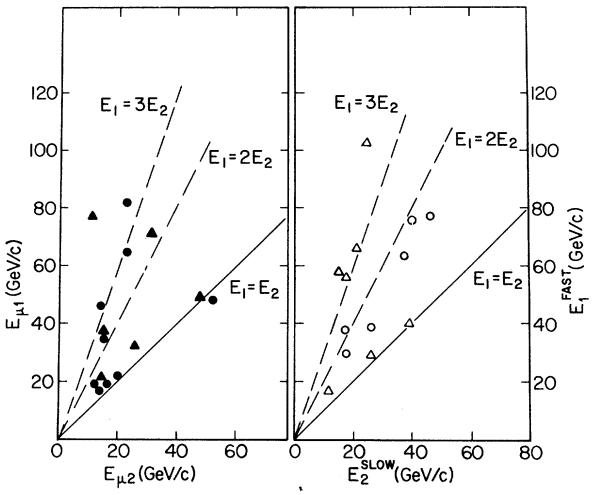

FIG. 2. Scatter plot of the energy of the members of a dimuon of opposite sign (left) and of same sign (right). Circles correspond to incident μ^+; triangles, to incident μ^-. The lines $E_1 = nE_2$ are drawn to guide the eye.

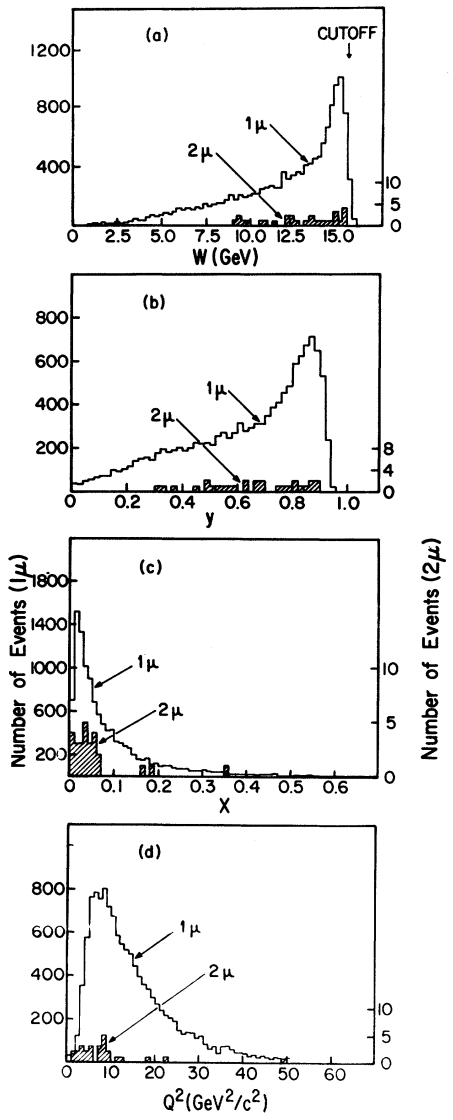

FIG. 3. Histograms of single-muon and dimuon events. (a) Invariant recoil mass, W; (b) fractional energy of virtual photon, y; (c) scaling variable x; and (d) four-momentum transfer squared, q^2.

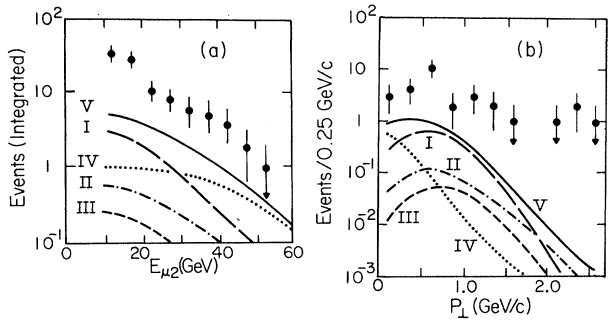

FIG. 4. (a) Integral energy spectrum of the slowest dimuon member (number of events with $E_{\mu_2} > E$). (b) Transverse-momentum (differential) distribution relative to the virtual-photon direction of the slowest diumuon member. Various background components are shown: decay μ from π and K in the hadronic cascade following the μ interaction (I), prompt μ from the initial interaction via conventional processes (II), prompt muons produced by the hadronic cascade (III), QED tridents with one muon undetected (IV), and total background (V). Errors shown are statistical errors only.

the graphs due to an ambiguity in E_{μ_1} measurement. In Figs. 4(a) and 4(b) are shown, respectively, the (integrated) energy distribution of the produced μ and the (differential) transverse momentum measured with respect to the virtual-photon direction.

In summary, the most striking features of the 2μ events as exhibited by the raw data are as follows: (1) $E_{\mu_1} > E_{\mu_2}$ in opposite-sign pairs; (2) no charge preference of the produced muon; (3) apparent threshold in the invariant mass W; (4) "flat" p_T distribution up to 2.6 GeV/c, dN/dp_T $\sim \exp(-2p_T)$; (5) no observed peak in the apparent mass; (6) $\langle x \rangle_{2\mu} = 0.05$ vs $\langle x \rangle_{1\mu} = 0.11$; (7) $\langle q^2 \rangle_{2\mu} = 7.5$ (GeV/c)^2 vs $\langle q^2 \rangle_{1\mu} = 15.0$ (GeV/c)^2; and (8) copious hadron production as seen in the iron-scintillator target array.

The multimuon events are unlikely due to π or K decays. This is indicated by the expected low p_T values of decay muons and the small acceptance of the apparatus at low p_T. A Monte Carlo calculation confirms this.

The target-detector geometry and magnetic field are included in all relevant details. The muon-nucleus interaction is simulated using experimentally measured inclusive hadron production distributions[5] at 150 GeV and a charged hadron multiplicity (W and q^2 dependent) from lower-energy electroproduction.[6] Kaon production is assumed to follow the same inclusive distribution as for pions but with 1/10th of the multiplicity. The particles produced in the initial interaction are allowed to interact further in the target and produce more secondary hadrons. This cascade process is continued through the entire apparatus down to sufficiently low energy of the participating particles.[7] The scattered muon and the decay muons are likewise traced through the apparatus.

The hadrons participating in the cascade shower can produce "prompt" muons, and this component has been evaluated using fits of single-μ production of protons on nuclei at 200 GeV/c and below.[4] Likewise the virtual photon can be expected to produce prompt muons from conventional sources

(e.g., vector mesons). To estimate this component it is assumed that such prompt muons and pions are produced in the same ratio as observed in hadron-hadron collisions. (To the extent that prompt μ's are emitted pairwise their contributions are overestimated.) Background muons from electromagnetic tridents can be produced, viz., a Bethe-Heitler, bremsstrahlung, or deep Compton production process.[8] The apparatus is biased severely against QED processes which occur mostly at low four-momentum transfers of the virtual photon or muon propagators. In addition, to be observed as 2μ events, one of the trident members must escape detection either due to its low energy or its large angle ($\theta_2 \gtrsim 200$ mrad). In a separate Monte Carlo calculation, the 2μ yield from QED (coherent and incoherent elastic) tridents surviving the experimental cuts is calculated.[9] The background calculations are summarized in Fig. 4. Other processes may contribute at a far lower rate: QED events from μe scattering, muon production via Lee-Wick bosons, intermediate vector bosons,[10] or Bethe-Heitler heavy-lepton pairs.[11] The total background discussed here is about 4.9 events. Therefore, most multimuon final states do not appear to come from readily identifiable sources.

The abundance of dimuons and trimuons as well as the kinematic distributions suggest the production and decay of heavy particles in deep inelastic muon interactions.[1,12] It should be noted that the measurement of the production cross section of heavy particles permits the evaluation of the contribution to deviations from Bjorken scaling at $x < 0.1$. However, it is presently far from clear whether this could fully explain the observed scale-breaking effects in deep inelastic muon scattering.[2,3,13]

The net total of 27 dimuon events yield a cross section—*uncorrected for acceptance*—of 5×10^{-36} cm^2/nucleon for the process $\mu N \to \mu\mu X$. The requirement that the fastest dimuon member be the triggering particle provides the *uncorrected rate* of 2μ production relative to the number of observed single muon events: $\sigma(\mu N \to \mu\mu X)/\sigma(\mu N \to \mu X) = 5\times10^{-4}$. The above values and the various distributions presented here are strongly dependent on the acceptance of the apparatus. The present results can be extrapolated to predict the total cross section and the distributions in terms of the various kinematical variables only by assuming a definite model.[14]

It is a pleasure to acknowledge the assistance of the staff of Fermilab during the data-taking phase. We thank A. Kotlewski, L. Litt, L. Hand, S. Loken, M. Strovink, and W. Vernon for their early contributions to this work. This work was supported in part by the National Science Foundation under Grant No. GP29070 and by the U. S. Energy Research and Development Administration.

[1]K. W. Chen, in *Proceedings of the International Conference on New Particles with New Quantum Numbers, Madison, Wisconsin, 1976*, edited by D. B. Cline and J. J. Kalono (Univ. of Wisconsin Press, Madison, Wis., 1976).

[2]Y. Watanabe *et al.*, Phys. Rev. Lett. 35, 898 (1975).

[3]C. Chang *et al.*, Phys. Rev. Lett. 35, 901 (1975).

[4]K. J. Anderson *et al.*, Phys. Rev. Lett. 36, 237 (1976), and 37, 799 (1976); J. G. Branson *et al.*, Phys. Rev. Lett. 38, 457 (1977).

[5]W. A. Loomis *et al.*, Phys. Rev. Lett. 35, 1483 (1975). The expression of the inclusive distribution cited for $0 < x' < 1$ is used. For $1 < x' < 0$, an expression that fits the lower-energy electroproduction data is used.

[6]P. H. Garbincius *et al.*, Phys. Rev. Lett. 32, 328 (1974).

[7]A. Van Ginneken, Fermilab Report No. FN-272, 1975 (unpublished).

[8]S. Brodsky and S. Ting, Phys. Rev. 145, 1018 (1966); P. Kessler, Acta Phys. Austriaca 41, 141 (1975), and Nuovo Cimento 53, 809 (1960).

[9]The total cross section for other QED processes is much smaller while differences in acceptance are highly unlikely to promote their contribution to a large fraction of the observed total [cf. C. Carimalo *et al.*, Phys. Rev. D 10, 1561 (1974)]. We thank S. Brodsky for providing us with his trident program.

[10]R. W. Brown and J. Smith, Phys. Rev. D 3, 207 (1971); R. Linsker, Phys. Rev. D 5, 1709 (1972); H. Fearing, M. Pratap, and J. Smith, Phys. Rev. D 5, 158 (1972).

[11]Y. S. Tsai, Rev. Mod. Phys. 46, 813 (1974). The possibility of heavy-lepton production at the muonic vertex is not considered here.

[12]A. De Rújula, in Proceedings of the 1976 Coral Gables Conference, Miami, Florida, 1976 (unpublished); S. L. Glashow, in *Proceedings of the International Conference on New Particles with New Quantum Numbers, Madison, Wisconsin, 1976*, edited by D. B. Cline and J. J. Kalona (Univ. of Wisconsin Press, Madison, Wis., 1976); J. Pati and A. Salam, International Center for Theoretical Physics, Trieste, Report No. IC/76/63, 1976 (to be published); F. Bletzacher, H. T. Nieh, and A. Soni, Phys. Rev. Lett. 37, 1317 (1976); V. Barger and R. J. N. Phillips, Phys. Rev. Lett. 65B, 167 (1976); S. Nandi and H. Schneider, Phys. Rev. D 15, 3247 (1977); L. Baulieu and C. Piketty, Nucl. Phys. B120, 333 (1977); D. P. Roy, Tata Institute Report, 1977 (to be published); H. D. Politzer, Harvard University Re-

port No. HUTP-77/A001, 1977 (to be published).
[13]H. Anderson *et al.*, in *Proceedings of the Eighteenth Conference on High Energy Physics, Tbilisi, U. S. S. R., 1976,* edited by N. N. Bogolubov *et al.* (The Joint Institute for Nuclear Research, U.S.S.R., 1977).
[14]Barger and Phillips (Ref. 12) estimate on the basis of a charm-production model, that the corrected rate for $\sigma(2\mu)/\sigma(1\mu)$ is 0.5×10^{-2}.

Classification of Yang-Mills Fields

Moshe Carmeli[a]
Department of Physics, Ben Gurion University of the Negev, Beer Sheva 84120, Israel
(Received 31 May 1977)

A classification of the Yang-Mills fields is presented using spinor methods. Each class of fields is associated with certain values of five invariants, of which four are complex and one is real. The whole classification is described in terms of two diagrams.

In this Letter I give a classification of the classical Yang-Mills fields along with their invariants using spinor methods.[1] Two diagrams are consequently presented that describe the classification. Not only the problem of classification of gauge fields is of interest per se, but it is of considerable importance in obtaining exact solutions of the Yang-Mills field equations. This fact is well-known in general-relativity theory.

The problem of classifying the Yang-Mills fields has recently been discussed using the method of infinitesimal holonomy group.[2] As has been pointed out[2] the classification obtained in this method, however, is not gauge invariant. Hence the physical meaning of such a classification is not clear since one class of fields can be transferred into another by a guage transformation. My method of classification is invariant under the product of the space-time and gauge groups. This group is taken here as $SL(2,C)\otimes SU(2)$.

The invariants and the classification[3] of the Yang-Mills fields were also discussed using the vector methods.[4] A total of nine real invariants were found that describe a complete set of independent invariants. However, the method proved to be useless for the classification problem. The eigenvalue-eigenvector calculation becomes so cumbersome that computer use was needed without achieving the desired classification. The problem of classification was thus left unsolved. It was pointed out, however, that three types of different fields can be isolated and associated with different values of the invariants. These are those fields for which (1) all invariants are different from each other; (2) all invariants are zero; or (3) the invariants satisfy a certain algebraic relation between themselves. It is well known, however, that when the invariants satisfy a certain relation between themselves, it is not necessary that one obtain only one kind of field. Both the electromagnetic and the gravitational fields are of such nature. For example, when all invariants of the gravitational fields vanish, one obtains three different types of fields rather than just one. In the Yang-Mills case the situation is even more complicated because of the double group structure. I show in the following that one has exactly six independent relations between the invariants (see Figs. 1 and 2) rather than the three relations that were pointed out using the vector method.[4] I also show that associated with these relations between the invariants there are exactly twelve independent and physically different types of Yang-Mills fields (see Figs. 1 and 2), rather than the only three fields found so far.[4] I thus have a complete and maximally detailed classification of the Yang-Mills

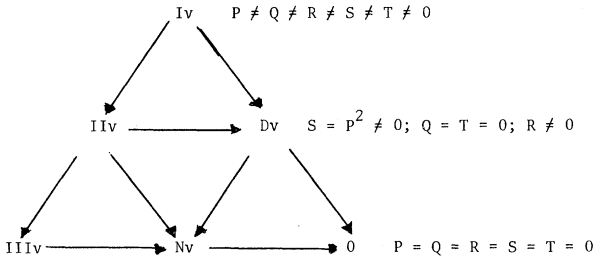

FIG. 1. Isovector diagram of classification. An arrow $A\rightarrow B$ indicates that type-B field is obtained from type-A field. The symbols in the diagram are as follows: $\mathrm{Iv}=\chi_{AB\dot{k}}$; $\mathrm{IIv}=\alpha_{(A}\beta_{B)\dot{k}}$; $\mathrm{Dv}=\alpha_{(A}\beta_{B)}\gamma_{\dot{k}}$; $\mathrm{IIIv}=\alpha_{(A}\alpha_{B)\dot{k}}$ (where $\alpha_{B\dot{k}}$ is defined by $\alpha_{B\dot{k}}\alpha_{C\dot{k}}=\alpha_B\alpha_C$); $\mathrm{Nv}=\alpha_{(A}\alpha_{B)}\gamma_{\dot{k}}$; and 0 is the zero field (included for completeness). If one chooses the vector $\gamma_{\dot{k}}$ in case Dv to be real then in addition to satisfying the conditions indicated in the diagram it satisfies $R=P\bar{P}$.